# 300 Nights of Science with IGRINS at McDonald Observatory

Gregory N. Mace[a], Hwihyun Kim[a,b], Daniel T. Jaffe[a], Chan Park[b], Jae-Joon Lee[b], Kyle Kaplan[a], Young Sam Yu[b], In-Soo Yuk[b], Moo-Young Chun[b], Soojong Pak[c], Kang-Min Kim[b], Jeong-Eun Lee[c], Chris Sneden[a], Melike Afşar[d], Michael Pavel[a], Hanshin Lee[a], Heeyoung Oh[b], Ueejeong Jeong[b], Sunkyung Park[c], Ben Kidder[a], Hye-In Lee[c], Huynh Anh Nguyen Le[c], Jacob McLane[a], Michael Gully-Santiago[e], Jae Sok Oh[b], Sungho Lee[b], Narae Hwang[b], and Byeong-Gon Park[b,f]

[a]Department of Astronomy and McDonald Observatory, University of Texas at Austin, 2515 Speedway, Stop C1400, Austin, Texas 78712-1205, USA
[b]Korea Astronomy and Space Science Institute, 776 Daedeokdae-Ro Yuseong-Gu Daejeon, 34055 Republic of Korea
[c]School of Space Research, Kyung Hee University, 1732, Deogyeong-Daero, Giheung-Gu, Yongin-Si, Gyeonggi-Do 17104, Republic of Korea
[d]Department of Astronomy and Space Sciences, Ege University, 35100 Bornova, Izmir, Turkey
[e]Kavli Institute for Astronomy and Astrophysics, Peking University, Yi He Yuan Lu 5, Haidian Qu, 100871 Beijing, Peoples Republic of China
[f]University of Science and Technology, 217 Gejeong-Ro Yuseong-Gu Daejeon, 34113 Republic of Korea

## ABSTRACT

The Immersion Grating Infrared Spectrometer (IGRINS) is a revolutionary instrument that exploits broad spectral coverage at high-resolution in the near-infrared. IGRINS employs a silicon immersion grating as the primary disperser, and volume-phase holographic gratings cross-disperse the H and K bands onto Teledyne Hawaii-2RG arrays. The use of an immersion grating facilitates a compact cryostat while providing simultaneous wavelength coverage from 1.45 - 2.5 $\mu$m. There are no cryogenic mechanisms in IGRINS and its high-throughput design maximizes sensitivity. IGRINS on the 2.7 meter Harlan J. Smith Telescope at McDonald Observatory is nearly as sensitive as CRIRES at the 8 meter Very Large Telescope. However, IGRINS at R≈45,000 has more than 30 times the spectral grasp of CRIRES* in a single exposure. Here we summarize the performance of IGRINS from the first 300 nights of science since commissioning in summer 2014. IGRINS observers have targeted solar system objects like Pluto and Ceres, comets, nearby young stars, star forming regions like Taurus and Ophiuchus, the interstellar medium, photodissociation regions, the Galactic Center, planetary nebulae, galaxy cores and super novae. The rich near-infrared spectra of these objects motivate unique science cases, and provide information on instrument performance. There are more than ten submitted IGRINS papers and dozens more in preparation. With IGRINS on a 2.7m telescope we realize signal-to-noise ratios greater than 100 for K=10.3 magnitude sources in one hour of exposure time. Although IGRINS is Cassegrain mounted, instrument flexure is sub-pixel thanks to the compact design. Detector characteristics and stability have been tested regularly, allowing us to adjust the instrument operation and improve science quality. A wide variety of science programs motivate new tools for analyzing high-resolution spectra including multiplexed spectral extraction, atmospheric model fitting, rotation and radial velocity, unique line identification, and circumstellar disk modeling. Here we discuss details of instrument performance, summarize early science results, and show the characteristics of IGRINS as a versatile near-infrared spectrograph and forerunner of future silicon immersion grating spectrographs like iSHELL[2] and GMTNIRS.[3]

**Keywords:** spectrograph, silicon immersion grating, high resolution, infrared optics, optomechanics, broad-band coverage, near-infrared, H2RG array, young stellar objects, Giant Magellan Telescope

E-mail: gmace@astro.as.utexas.edu, Telephone: +1 512 471 3853
*More than 3 times the spectral grasp of the CRIRES$^+$ upgrade[1]

## 1. INTRODUCTION

Infrared instrumentation lets us peer into the cool and dust-obscured parts of the universe, and infrared spectroscopy unfurls the source flux so we can determine physical properties. The Immersion GRating INfrared Spectrometer (IGRINS) is the premier infrared spectrograph available to the astronomical community and a precursor to future silicon immersion grating spectrographs like iSHELL[2] and GMTNIRS.[3] We are using IGRINS to investigate the initial stages of star formation deep within molecular clouds, energy states of the interstellar medium, cluster membership of cool stars, the formation history of the Milky Way, and the composition of evolved stars.

In the past, infrared spectrograph designs were optimized for either large spectral grasp *or* high resolution. We can overcome small detector formats with echelle gratings, which disperse spectral orders in the spatial direction, but pixel sampling still limits wavelength coverage at high resolution. Prior to IGRINS, NIRSPEC[4] at Keck Observatory provided the broadest spectral coverage (∼30% that of IGRINS, but without order overlap) at high resolution. The diversity of near-infrared science cases in astronomy has motivated many spectrograph designs that include cryogenic mechanisms. However, adjustable instruments have drawbacks because simultaneous observations at all wavelengths are not possible, the echellogram placement is not completely repeatable, and the instrument cost increases when engineering is increased. IGRINS circumvents these design pitfalls by using a silicon immersion grating and transmissive volume-phase holographic gratings to capture the entire 1.45-2.5 $\mu$m spectrum at high-resolution with a single instrument configuration.

We previously reported the design and early performance of IGRINS,[5,6] which is briefly summarized here. IGRINS was built as a partnership between the University of Texas (UT) at Austin and the Korea Astronomy and Space Science Institute (KASI). At the heart of IGRINS is the silicon immersion grating developed at UT Austin.[7,8] By immersing light in silicon and reflecting it off the inside of the ruled surface, the dispersion is amplified by the index of refraction (n≈3.4 for silicon at 130K[9]). The result is that light longward of the ∼1.1 $\mu$m absorption cutoff of silicon is dispersed to high-resolution in a fraction of the distance of a similar spectrograph under vacuum. This produces a substantial cost reduction in the instrument design as the volume of the cryostat is reduced. Additionally, the judicious selection of slit length, beam size, spectral resolution, and camera f-number have allowed us to fit the entire H- and K-band echellograms onto a pair of 2048×2048 Teledyne H2RG HgCdTe arrays. The result of this design is an unprecedented R≈45,000 spectrum of both the H and K bands (1.45-2.5 $\mu$m), simultaneously. To put this spectral grasp in context, this is more than 30 times the wavelength coverage of CRIRES[10] and 3 times the coverage of the CRIRES$^+$ upgrade[1] at a similar resolution. Furthermore, the high throughput of IGRINS yields a similar sensitivity to its closest analog, the NIRSPEC spectrograph on the 10m Keck II telescope, and does so with 3 times the spectral range, no gaps in wavelength coverage, and with much less telescope collecting area.

As of May 2016, IGRINS has completed more than 300 nights of TAC (Telescope Allocation Committee) awarded science on the Harlan J. Smith 2.7m telescope at McDonald Observatory, which is nearly half of all the nights awarded in the last two years. Published papers cover broad science topics including a FU Ori type star HBC 722,[11] the detection of low-mass companions to high-mass stars,[12] the discovery of new elements in planetary nebulae,[13] state-of-the-art estimates of chemical composition of very metal-poor stars,[14] characteristics of jets around LkHa 234,[15] circumstellar disk modeling of Class I Young Stellar Objects,[16] the discovery of Neptune sized planets in the Hyades Star Cluster and Upper Scorpius,[17,18] a super-Earth in the vicinity of the Pleiades,[19] and evidence of a 2 Myr old exoplanet orbiting a classical T Tauri star.[20]

### 1.1 IGRINS Updates Since Commissioning

Since we reported on the early performance of IGRINS for the first two commissioning runs in March and May 2014,[6] we have had two summer maintenance periods where IGRINS was modified in the lab at UT Austin, one vacuum failure at the observatory, and a number of software adjustments for data acquisition and analysis. Each milestone is discussed below.

In July and August 2014, between commissioning and regular science operations, we maintained IGRINS in the lab at UT Austin. During this maintenance we replaced Cernox temperature sensors, tested ThAr and UNe arclamps, and added baffling inside the cryostat to address a K-band light leak. We also used this lab time to

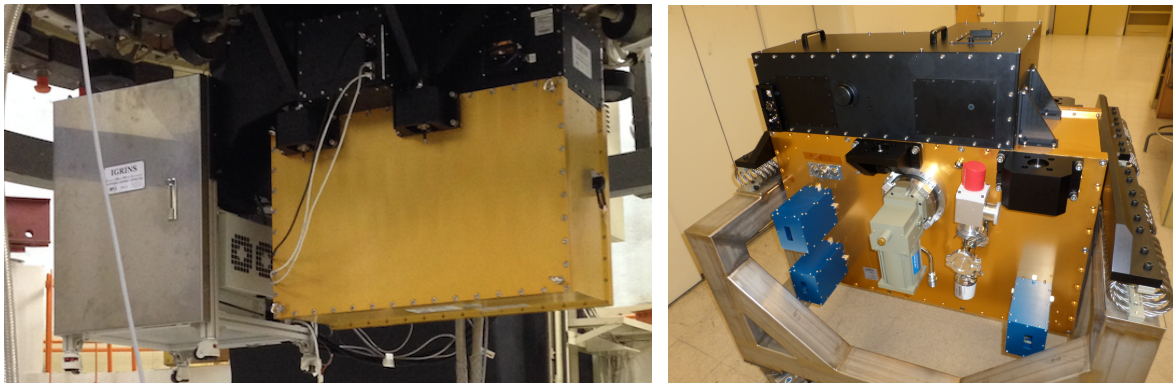

Figure 1. Left: IGRINS (gold colored cryostat and gray electronics rack) mounted on the 2.7m Harlan J. Smith Telescope at McDonald Observatory. Right: IGRINS on the transportation cart with the calibration unit mounted on the top, the CTI 1050 coldhead located in the center (green) and the JADE2 detector interface cards for the two spectral detectors and the slit-viewing camera (covered by the blue boxes). The long dimension of the cryostat is only 0.96m.

test detector readout schemes and to train the team on the instrument mechanics and software. The second summer maintenance was in August 2015. This time we replaced the CTI 1050 two-stage refrigerator system with a spare, baked the getter, and added more baffling around the K-band detector. The additional baffling reduced the K-band light leak from ∼0.23 counts per second per pixel to ∼0.09 counts per second per pixel.

On 18 May 2015 IGRINS experienced a vacuum failure while at McDonald Observatory. During a routine vacuum refresh, in which IGRINS is warmed and pumped for a day and then cooled back down, power was lost to the observatory. The vacuum pump allowed air to backflow until the cryostat was at $10^{-4}$ torr, up from the standard on-pump level of $10^{-8}$ torr. This failure was amplified because IGRINS had been left on the vacuum pump while cooling and the cryostat was colder than 200K. The vacuum valve was closed only after the backflow had occurred. Once power was restored to the observatory, IGRINS was warmed to room temperature while on the vacuum pump. We initially monitored the instrument by closing the valve and logging the internal pressure, which rose from $10^{-5}$ to $10^{-3}$ torr in two hours. This implied a vacuum leak or significant out-gassing in the cryostat. To remove locked-in gasses, we set the internal heaters to 300K and left IGRINS on the vacuum pump for two days. After the pressure had stabilized at $10^{-6}$ torr, we tested the detectors at room temperature and found that they operated normally. We then installed IGRINS on the telescope and cooled IGRINS to normal operating temperatures (125K for the optical bench, 130K for the immersion grating, and ∼65K for the detectors). This cooldown took 48 hours, which is longer than the usual 30 hours, but we were back on-sky without any lost observing time. Fortunately, nothing was damaged by this vacuum failure event and we have adjusted our procedures to avoid it in the future.

Observing preparation, data acquisition, and data reduction software was developed before IGRINS was commissioned.[21,22] Our empirical tests of the signal-to-noise were about 84% what was initially predicted by the IGRINS Exposure Time Calculator,[6] and so the tool was updated to give observers correct estimates prior to observing[†]. Additionally, a Python based tool was created by UT graduate student Kyle Kaplan to create 2MASS K-band finder charts for any IGRINS slit orientation[‡]. The observing software for IGRINS, which is described below, has been adjusted for usability, improved guiding, and with additional off-slit guide star tools. Finally, the IGRINS data reduction Pipeline Package (PLP) has had a number of primary releases, uses ThAr arclamp and OH sky lines for the wavelength solution, and optimally extracts both 2D and 1D spectra for point and extended sources.[§]

Since commissioning, IGRINS has produced nearly 2 TB of spectral data (∼16.4 MB per FITS file), and the typical observing night produces ∼5GB of spectral data. Each night the spectral files are copied to a data

[†] http://irlab.khu.ac.kr/~igrins/
[‡] https://github.com/kfkaplan/igrins_observability
[§] https://github.com/igrins/plp

storage computer at McDonald Observatory, a storage computer at KASI in South Korea, and to the observers portable hard drive and/or institution. Once per observing run all files are copied to four additional external hard drives maintained by G. Mace and H. Kim, the IGRINS postdocs. In total, there are at least seven data backups in three different geographical locations.

### 1.2 IGRINS Observing

Observing with IGRINS at McDonald Observatory generally requires two people, one as a telescope operator and the other as the IGRINS observer. An experienced user can do both but, because IGRINS is a new instrument, many users need support. For the 300 nights of observation discussed here, support was primarily provided by G. Mace, H. Kim, and K. Kaplan.

At the beginning of each observing night we acquire dark, flat lamp, ThAr and UNe arclamp calibration frames. During twilight, the observer focuses the telescope and verifies telescope pointing on a bright star near the zenith. The 2.7m Telescope Control Software provides telescope control and information on science targets such as time of observation, target position, and target airmass. Once the telescope is slewed to a target, an image is taken in the K band with the IGRINS slit viewing camera. Employing the Slit Viewing Camera software package, the observer moves the target to a reference position near the slit. The standard slit position angle is 90° (in the east-west direction) but the observer can manually change this to any desired orientation. From the reference position, the observer can choose to guide on the target using the wings of the PSF that fall on the sides of the 1 arcsecond wide slit, or by using an off-slit guide star. Off-slit guiding is the most reliable because the full guide star PSF is available for determining the centroid location, but the ∼2×3 arcminute field-of-view of the slit view camera only permits off-slit guide stars about half of the time. After establishing guiding with the target on the slit, the observer uses the Data Taking Package to set H- and K-band exposure times and to nod the target along the slit. The minimum exposure time is 1.63 seconds for a single read. Yet, typical exposure times are 30-600 seconds because Fowler sampling with 16 reads requires exposure times >28 seconds. A Fowler-16 sampling rate was chosen based on the analysis of the MOSFIRE[23] H2RG detector.[24]

Although IGRINS observing time is scheduled classically, with an observer spending their time on the proposed science targets, IGRINS is a good queue instrument. Because IGRINS has no moving parts, every spectrum has the same format and resolution, and every observer gets the same spectrum. To avoid redundancy in popular observing programs (like the Orion, Taurus, and Ophiuchus star forming regions) we have established informal observing queues. The flexibility provided by the informal queue increases our weather related efficiency to ∼80%, compared to the ∼50% of purely classical observing. In August 2015 and March 2016 we held 4 night mini-queues where observers could request up to 2 hours of observations. These nights were ideal for completing exploratory, short, and end-of-project observations. Specifically, we targeted comets, spectroscopic binaries that needed multiple epochs across a week, exoplanet candidates, and nearby galaxies. Remote observing has also been used on occasions when observers were unable to travel to McDonald or very specific observations were required.

## 2. ON-TELESCOPE PERFORMANCE

There are a number of changes to the instrument sensitivity, relative to the baseline lab performance, when IGRINS is installed on the Harlan J. Smith Telescope at McDonald Observatory. One of these changes is the electronic isolation of the detectors. Finding a good ground has been difficult at the observatory, and electronic feedback produces pattern noise on the detector that is repeated on all 32 readouts. Fortunately, we are able to remove this pattern noise in the data reduction process. Dark noise is higher when IGRINS is on the telescope because of light leaks and variable thermal background in the K band. The spectral stability of IGRINS changes when it is mounted at the Cassegrain focus because the gravity vector changes for each target. In this section we quantify each of these sources of sensitivity loss.

As general background, we provide the reader with some information relevant to the following discussion. The IGRINS preliminary on-sky performance[6] and the characterization of the IGRINS detectors during commissioning[25] were previously reported. Using up-the-ramp sampling, we measure baseline dark currents of 0.0147 $e^-$/s and 0.0109 $e^-$/s in H and K, respectively. The full well capacity of the IGRINS H and K detectors is ∼45000 counts, and the detector gains are 2.05 $e^-$/count and 2.21 $e^-$/count in H and K. Hot pixels on the

science detectors have values between 2500-3300 counts in H and 2000-4000 counts in K. Even in the longest science exposures, 1200 seconds, the OH sky lines peak at 4000 counts and are well below the full well limit. Typically there are 150-600 target continuum counts per exposure, providing signal-to-noise ratios of 100-200 in an ABBA nodded quad of exposures.

### 2.1 Electronic and Light-Leak Noise

The proximity of the IGRINS electronics cabinet to the detector electronics creates electronic noise. We do not see pattern noise in the UT Austin lab because we are able to isolate the electronics well. At McDonald, we have had difficulty achieving good grounding and electronic isolation, and as a result pattern noise is seen across the rows of the detectors and duplicated across all 32 readout channels. The pattern is $\sim$10 counts in amplitude and is spread out as the Fowler number is increased. The residuals on the pattern subtraction are generally $\sim$3 counts, which is less than the read noise. Light leaks consistently impact the same regions of the detector and do not change with telescope pointing. In the K band the light leak is $\sim$0.09 counts per second, leaving $\sqrt{N}$ noise of $\sim$7 counts in a pair of subtracted 300 second exposures. This is about twice the dark noise and a dominant noise source for faint targets.

### 2.2 Dark Noise Characterization

Dark frames provide one of the most consistent measurements of IGRINS' well-being. Pseudo-dark frames with 30 second exposures are obtained nightly by commanding the calibration unit to place a mirror in front of the entrance window. The 30 second exposure time matches the nightly flat lamp exposures. The darks for IGRINS are not true dark frames because the mirror temperature matches the ambient facility temperature and adds thermal background to the dark frames at a low level. Once a trimester, we also take a series of dark frames with exposure times between 30 and 3600 seconds as a historical log of the dark current in each of the spectrograph detectors.

To characterize the long-term health of the IGRINS detectors we inspect all of the dark frames with the standard 30 second exposure time to find the population statistics (counts per pixel) across the detector. Figure 2 shows the number of counts per pixel in bins of 10 counts. The logarithmic scale on the vertical axis accentuates the population outliers because >99.8% of the pixels are in the peak. Additional peaks in the H band at $\pm$250 counts are due to unpaired hot and cold pixels in the bottom readout of the detector, a localized issue that minimally impacts science. Cosmic rays have values of $\pm$500-600 counts, and bad pixels have a variety of values populating the positive tail of the histogram. A nuance of Figure 2 is the broader peak in the K-band detector due to higher thermal background noise and fewer bad pixels.

#### 2.2.1 Noise for 300 Nights

We define the noise to be the standard error ($\sigma$) of the counts in each quadrant of the detector. The upper-left quadrant is the darkest on each detector and the best for tracking the dark current as a function of time. Detector defects and light leaks add to the noise in the other three quadrants and is traced as we monitor and remedy these issues. Looking at just the darkest quadrant, Figure 3 shows $\sigma$ for each Julian Day of IGRINS science observations. Small variations in $\sigma$ may be driven by the vacuum quality, but comparison to the local temperatures in west Texas reveals that the dark noise is directly correlated with the readout electronics temperatures. With the IGRINS electronics mounted next to the cryostat at the Cassegrain focus (Figure 1), the detector electronics are in equilibrium with the ambient conditions of the telescope dome. The H-band noise is dominated by variations in the readout electronics temperatures, but the K band is also impacted by the temperature of the pseudo-dark mirror and light leaks that were reduced during August 2015 (in the center of Figure 3).

#### 2.2.2 Dark Current and Read Noise

Although the read noise and dark current were quantified in the lab,[25] we have now verified these noise sources with IGRINS on the telescope. We determined $\sigma$ for the darkest quadrant of each dark frame with exposure times >60 seconds and fit a line to $\sigma$ as a function of exposure time. From the fit, the slope gives the upper limit to the dark current and the y-intercept provides the read noise. We find that for the H-band detector, the

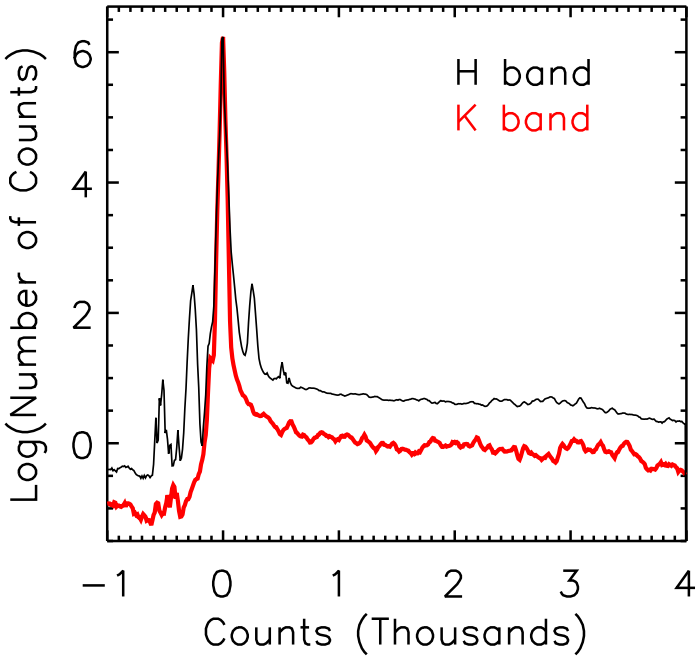


Figure 2. Histogram showing the number of pixels versus the number of counts in those pixels for a bin size of 10 counts. >99.8% of the pixels are in the peak, bad pixels populate the positive tail and minor peaks are due to coherent noise related to electronic interference.

read noise is ∼3.5 counts and the dark current is < 0.003 counts per second. The thermal background in the K band gives a higher limit for the dark current, <0.02 counts per second, but a similar read noise as in the H band, ∼3.5 counts.

### 2.3 Persistence

Detector persistence is common to H2RG detectors,[26,27] is unique to each device[¶], and is temperature dependent. During commissioning we identified the H-band detector as having stronger persistence than the K band. We tested the persistence of ThAr and flat lamp spectra at 65, 70, and 75K. Figure 4 shows that at 65 and 70K the K band has no measurable persistence, while at 75K the persistence after 2 minutes was <0.2% of the source flux (∼4 counts). We also found that at 75K the flat lamp caused less persistence than the ThAr arclamp, despite the same peak flux counts. As a result of these tests we decided that 65K is the best operating temperature for both detectors. After ∼5 minutes the persistence in both bands is <0.2% of the source flux (∼4 counts for our brighter targets).

### 2.4 Spectral Stability

Changes in the gravity vector on IGRINS causes flexure of the optics and impacts the placement of the echellograms. However, flexure is not the only source of variability in the echellogram placement. We are generally not interested in the spatial (vertical) changes in the spectral format because nightly flat lamp calibration identifies the order edges to within a pixel. The spectral (horizontal) changes in the echellogram are critical to science quality and so we have measured their stability for the first 300 nights of IGRINS science.

[¶] https://www.eso.org/sci/meetings/2009/dfa2009/Presentations/Finger_Wednesday_09_20.ppt

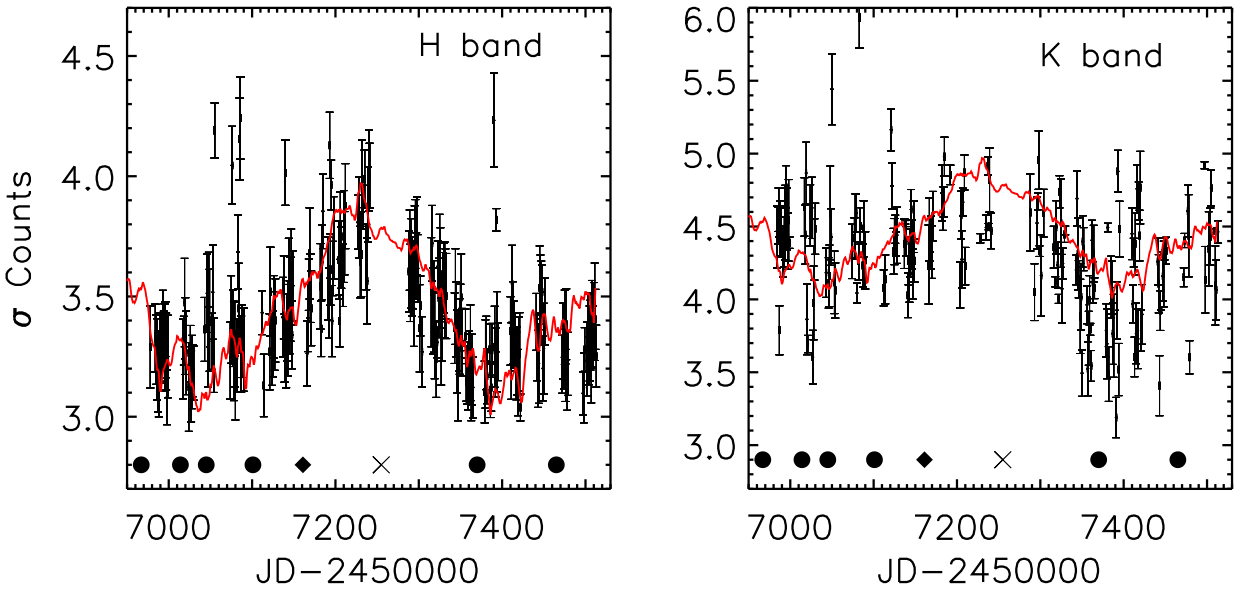


Figure 3. The standard error ($\sigma$) of the counts in dark frames for each Julian Day of IGRINS observations. Symbols along the bottom of the figure mark dates where we warmed IGRINS and refreshed the vacuum (circles), performed summer maintenance in the lab (X), and the May 2015 vacuum failure (diamond). The average temperatures in west Texas are included (red line), peaking in July 2015 at 32C and falling to -3C in February 2015 and 2016. There is no question that ambient temperatures impact dark noise.

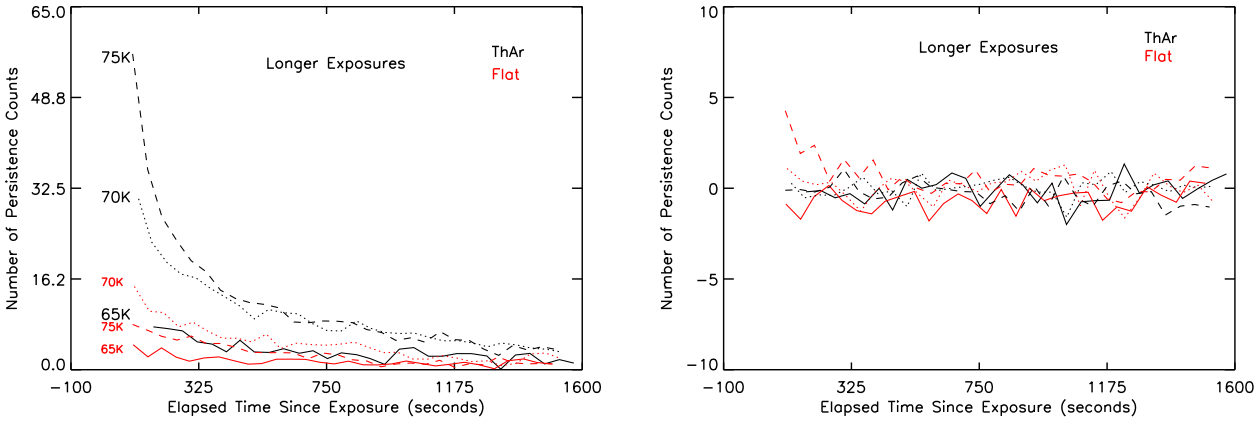


Figure 4. Left: H-band persistence (number of counts) for various detector temperatures and light sources. Right: Persistence in the K-band detector at temperatures below 75K is consistent with zero. Line styles are the same as for the H band. In both detectors the persistence is lower at lower temperatures.

### 2.4.1 Nightly and Weekly Stability

A 300s sky frame is shown in Figure 5 for both detectors along with 16 telluric lines that are tracked to measure spectral stability. The OH emission lines, and $H_2O$ absorption lines at the red end of the K band, provide a reliable measure of wavelength vs. pixel as a function of time. For every on-sky frame taken with IGRINS we vertically collapsed the box's shown in Figure 5 using a median filter, interpolated the spectrum to 100th of a

Table 1. Noise Budget for IGRINS Detectors when On Sky

| **Noise Source** | **H band & K band Noise** |
|---|---|
| Electronic | ∼3 counts per subtracted pair |
| Light Leaks | 0.09 counts per second, or ∼7 counts per pair of 300s exposures |
| Dark Current | $< 0.003$ in H & $< 0.02$ counts per second in K |
| Read Noise | ∼3.5 counts per exposure |
| Persistence | <0.2% source flux (∼4 counts) at 65K |
| **Total** | <12 counts per pixel per subtracted pair of exposures |

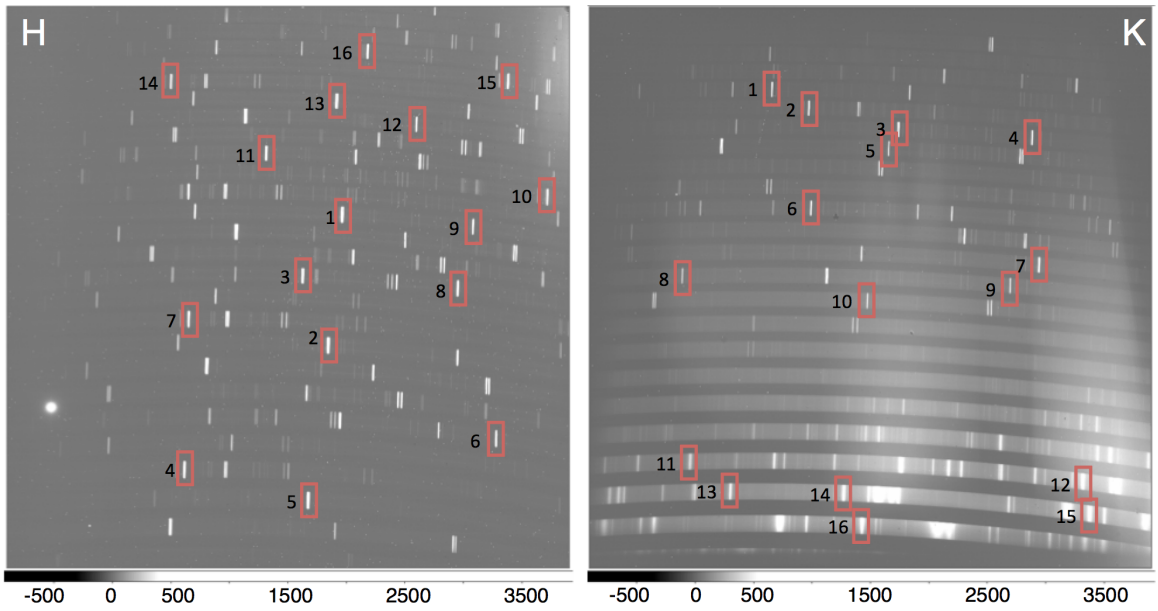


Figure 5. H and K band 300 second night sky spectra showing the boxes used to measure spectral stability. Also seen here are detector defects (circle and bad pixels in the H-band detector), thermal leakage from the detector electronics (upper right of H, lower right of K), and light leaks (center and right side of K).

pixel, and fit a Gaussian to the line in order to determine the line location. The result is 0.01 pixel precision on the relative line locations for all 300 nights (∼1,000 measurements each night for each detector).

The first question that we can answer is whether the echellogram has translated or rotated. Rotation would manifest as line locations moving is separate directions at opposing sides of the detectors. We do not see this. Instead, all boxes show the same relative offsets within the nightly uncertainties. This means that there is no rotation and that shifts in the echellograms are spatial or spectral translations.

The relative line locations for October and November 2015 observing runs are shown in Figure 6. Nightly variations are ∼0.1 pixels in the H band and ∼1 pixel in the K band, which is the expected flexure amplitude based on the instrument design.[5,6] The shape of the H-band flexure across a night reflects the observing program, producing '∪', 'N', and '∩' patterns as the observer follows a cluster or changes the slit position angle. These same patterns are seen in the K band, but with a larger amplitude. The gap in the K-band line position is real, and corresponds to the meridian crossing of the telescope (negative values occur when the target is located to the east of the meridian and positive when the telescope is pointed west). The diagonal lines reflect the observers preference for the Orion star forming region, which was observed for entire nights in November.

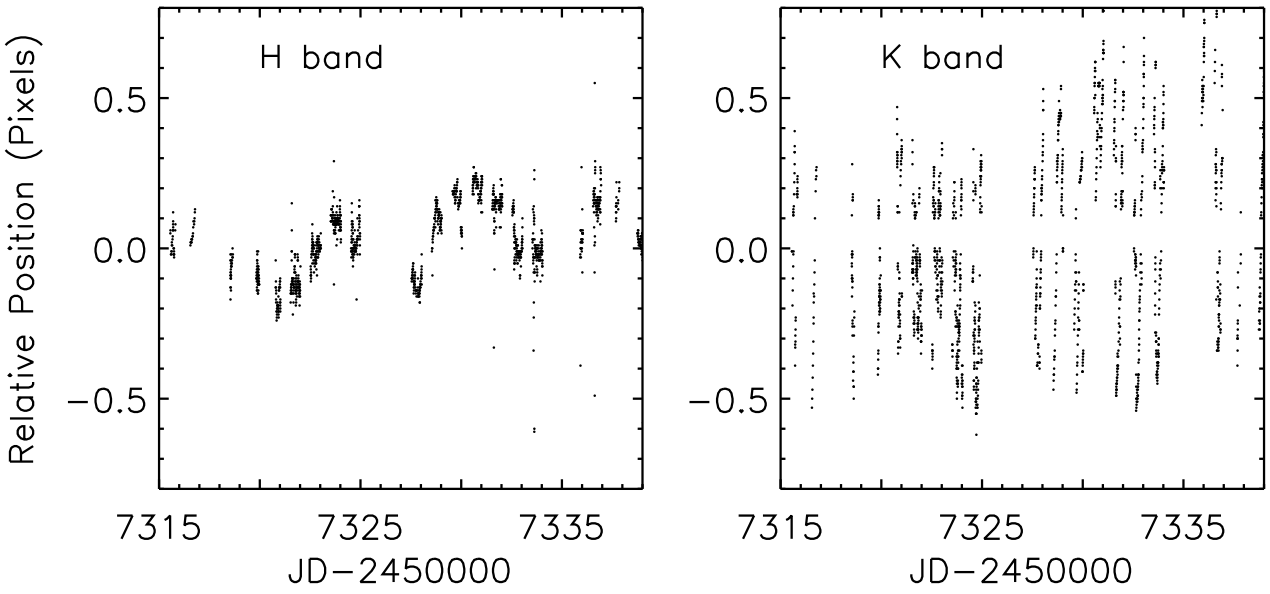


Figure 6. The relative location of OH emission lines on the detectors for a month centered around 1 November 2015.

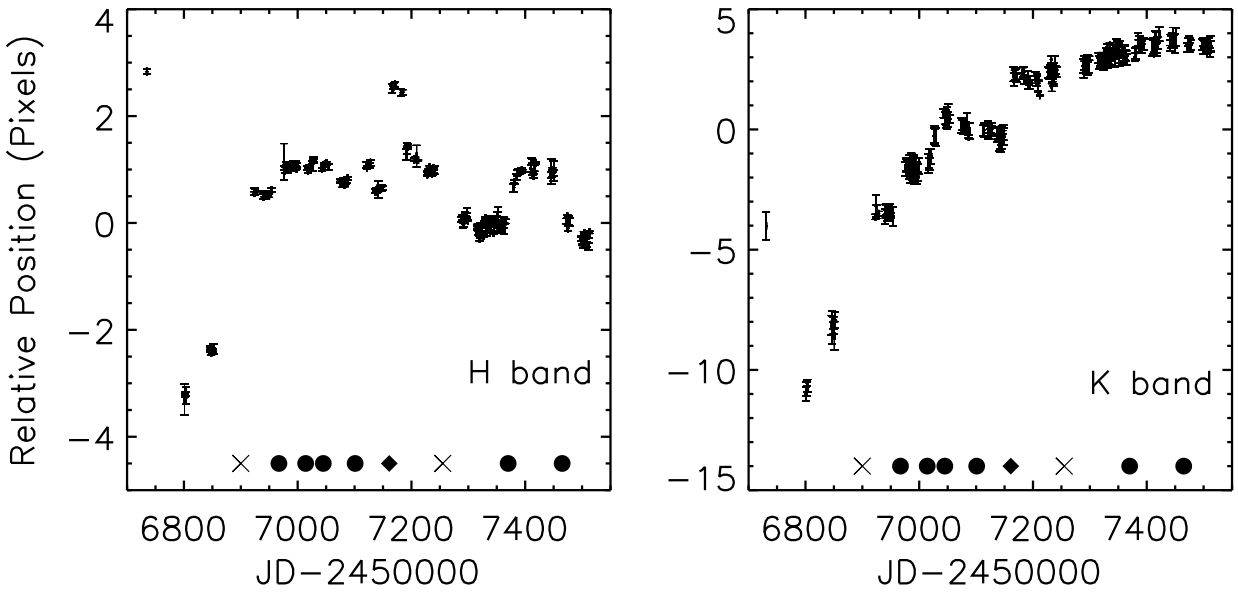


Figure 7. The relative location of OH emission lines for all IGRINS on-sky frames. Symbols are the same as in Figure 3.

### 2.4.2 300 Night Stability

Over longer periods of time, flexure is not the primary source of echellogram motion. Figure 7 shows the relative line locations for commissioning and all 300 science nights. The markers along the bottom of the figure are the same as in Figure 3 and identify the dates when the vacuum was refreshed, the May 2015 vacuum failure, and

regular summer maintenance. Between these milestones, the echellogram behaves as we see in Figure 6 with ambient temperature and gravity vector orientation dominating the flexure. We see a jump in the spectral format every time that IGRINS is taken off the telescope, thermal cycled for a vacuum refresh, or opened in the lab.

While inspecting the IGRINS slit mask during the summer of 2015, we found that it is able to move slightly within its retainer. This motion is greatest when IGRINS is warm and is the likely source of all the echellogram shifts seen in the H band. The vacuum failure had a clear impact on the echellogram placement, causing both the H and K to jump by about 2 pixels in the spectral direction. Prior to the summer 2015 maintenance, the K-band echellogram was continuously drifting. However, this drift has stabilized in the last year and is now comparable to the H band. As we discussed in the Introduction, in the summer of 2015 we adjusted the baffling around the K detector and may have stopped the drift by adjusting a fastener.

## 3. SCIENCE PERFORMANCE

IGRINS is ideal for sensitively measuring the characteristics of astronomical sources. The unmatched combination of throughput, spectral grasp, and fixed format allows observers to investigate the finest spectroscopic details. With continuous spectral coverage from 1.45 to 2.5 $\mu$m, R≈45,000, and optimal oversampling of 3.5 pixels, IGRINS outperforms all existing near-infrared echelle spectrographs in both wavelength coverage and throughput at a given resolution. It will not be supplanted by planned upgrades to competitors like CRIRES and NIRSPEC. Although the CRIRES and Phoenix[28] infrared spectrographs achieve higher resolution, their simultaneous spectral coverage is only a few to <1% that of IGRINS.

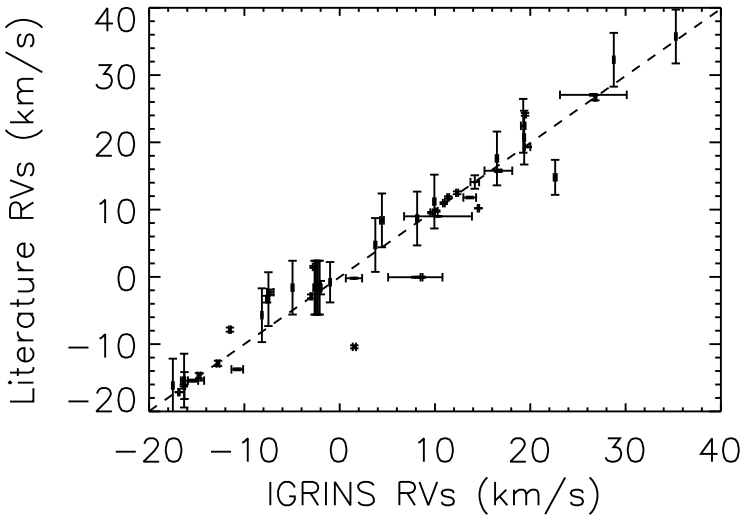


Figure 8. About a third of IGRINS targets have measured radial velocities in the literature. Overlap provides a check of our method and a zeropoint for determining absolute radial velocities. IGRINS uncertainties are an order of magnitude smaller than what is in the literature and outliers in this figure are likely binary stars.

### 3.1 Stellar Radial Velocities

Photometric surveys reveal the faintest members of the local universe, but radial velocities (RVs) are the missing component of most moving group studies. RVs precise to ∼1 km/s verify group membership, but RV precision lower than 200 m/s is required to find missing brown dwarf companions to stars.[29] Although exoplanet searches routinely achieve 1 m/s RV precision with dedicated instrumentation and small samples of bright stars, RV precision for many stars remains at the 1-2 km/s level. IGRINS is a revolutionary instrument for RVs because it has more than 20,000 resolution elements and a fixed spectral format. Each IGRINS resolution element is ∼7

km/s, but cross correlation of the entire spectrum provides relative RVs with uncertainties of 50 m/s (<1% of a resolution element). IGRINS RVs are verifying planet candidates around M dwarfs in the K2 campaign,[30] testing moving group membership for K and M dwarfs, and determining orbital solutions for spectroscopic binaries.

### 3.2 Stellar Parameters

With IGRINS' broad spectral coverage we measure stellar molecular abundances in high signal-to-noise ratio spectra.[14] Figure 9 shows the first CO overtone bandheads in the field red horizontal branch star HIP 54048 (blue) and the bright very metal-poor halo giant HD 122563 (black). Co-adding 16 CO lines with S/N>400 in the weak lined HD 122563 produces a median line profile with S/N>1000 and just a 3% line depth can differentiate abundances at 0.01 dex. Through comparison to MOOG synthetic atmospheres,[31] we also derive abundances in the near-infrared for Mg, Si, S, and Ca. Cooler evolved stars emit more light in the infrared than at optical wavelengths and IGRINS is a great tool for studying the dust-obscured evolved components of the galactic bulge.

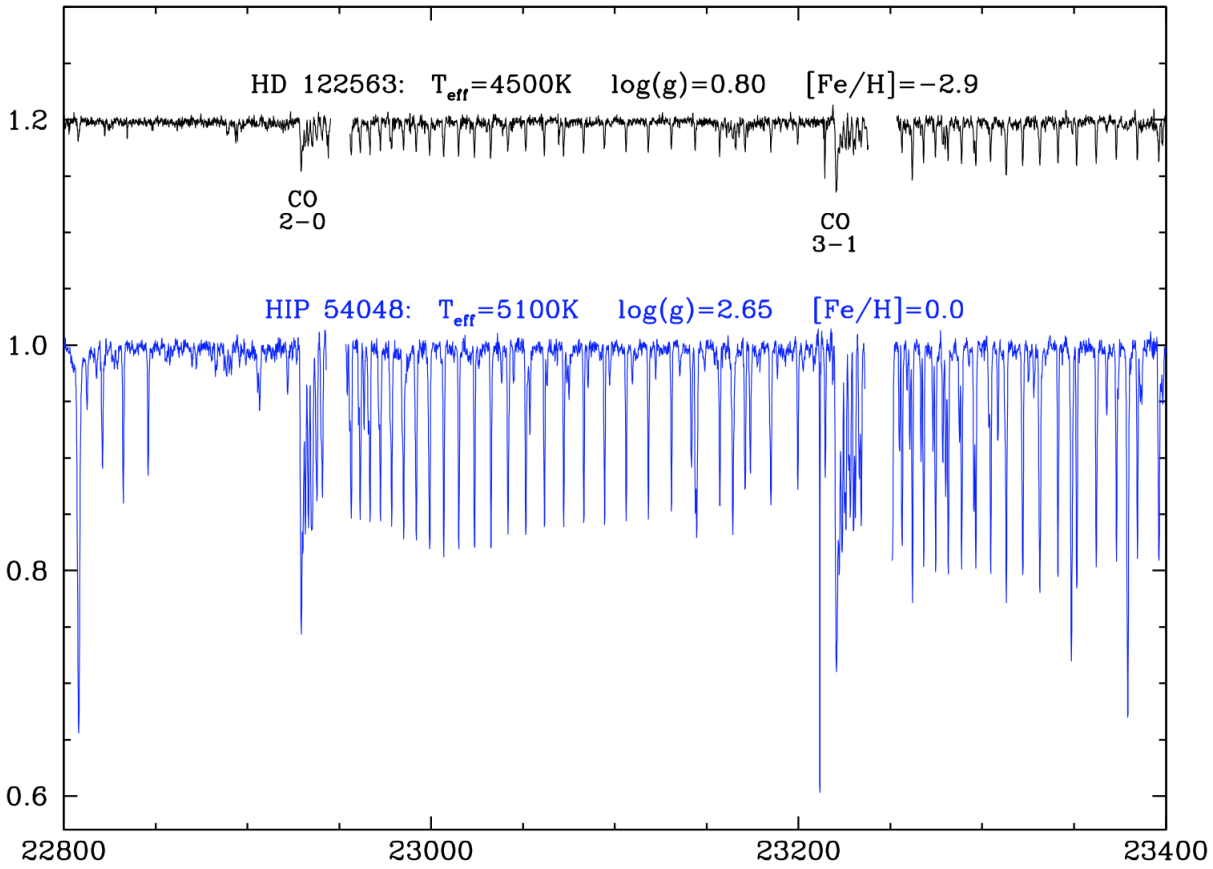


Figure 9. IGRINS spectra for HIP 54048 and HD 122563, evolved stars observed with IGRINS to calibrate infrared measurements of atmospheric abundances.[14]

### 3.3 The Interstellar Medium

Kaplan et al. (2016, in preparation) will present a detailed study of the $H_2$ excitation in the Orion Bar, which is a dense, nearby, and edge-on photo-dissociation region (PDR). Theories on the structure of the Orion Bar attempt to describe the morphology and energy states of the ionized, neutral and molecular components. The classic model depicts the Orion Bar as plane parallel slabs of gas and dust.[32] More recent models explain the energy populations of the gas by invoking a clumpy morphology,[33,34] variations in dust properties between PDRs and

the ISM,[35] or magnetic fields providing support against radiation pressure.[36,37] With the large spectral grasp and high resolution of IGRINS, Kaplan et al. have identified more than 80 hydrogen lines in a deep pointing on the Orion Bar. The energy transitions observed in the Orion Bar provide detailed information on gas physics, which is a probe of the density, ultra-violet radiation field, and the temperature of the molecular gas.

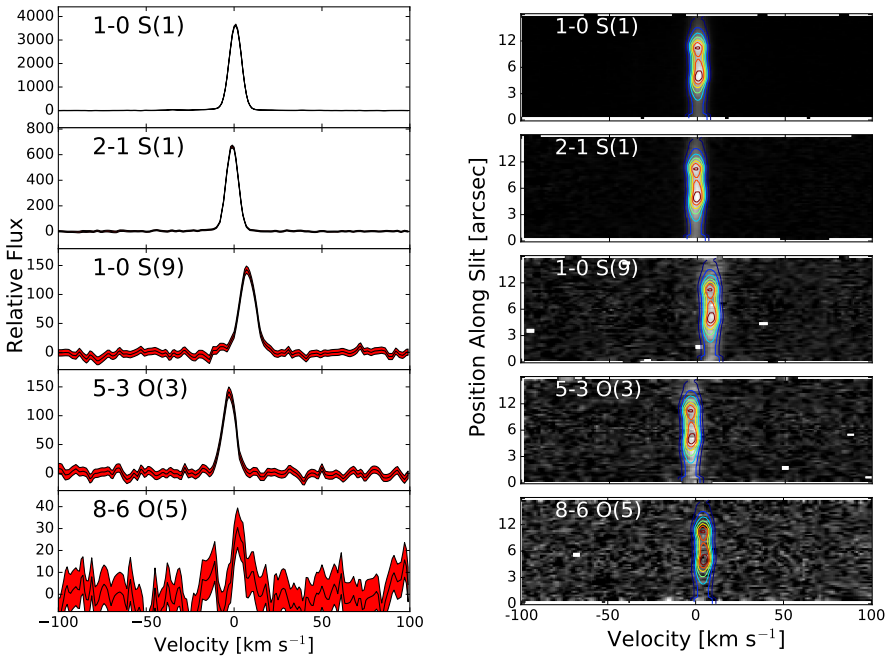


Figure 10. Examples of five position-velocity diagrams for $H_2$ rovibrational emission lines in the Orion Bar. The flux density in position-velocity space of the brightest line, 1-0 S(1), is used as a weighted template (colored contours) for extracting the flux of the other lines. The offsets in the velocity space are not physical but due to the limitation of theoretical line wavelengths.

## 4. THE FUTURE

In August 2016 IGRINS will return to UT Austin for annual maintenance, where we will continue to address light leakage and replace some hardware. We are making preparations to visit the Discovery Channel Telescope beginning in late-summer 2016. IGRINS has been awarded visiting instrument time on Gemini South in the 2018A semester. In conjunction with IGRINS, iSHELL[2] was developed for the NASA IRTF and will be commissioned in summer 2016. The capabilities of IGRINS and iSHELL are complementary, reducing the burden on astronomers to develop new data analysis tools, and yet differences in spectral coverage and resolution provide flexibility to science programs that utilize both instruments.

The most significant value of IGRINS is that it was designed and built as a prototype for the Giant Magellan Telescope Near-Infrared Spectrograph (GMTNIRS).[3,38,39] IGRINS grating development improved our silicon grating process[40,41] and fostered the UT and KASI collaboration. GMTNIRS will have many of the same H- and K-band capabilities as IGRINS, but will have five separate spectral channels to provide simultaneous coverage from ∼1.1-5 $\mu$m at high resolution. When commissioned on the Giant Magellan Telescope, GMTNIRS will obtain signal-to-noise >100 spectra for anything in the 2MASS[42] catalogs with 1 hour of exposure time.[43]

## ACKNOWLEDGMENTS

We acknowledge the hard working Observing Support Team at McDonald Observatory for their IGRINS support, especially Coyne Gibson, Cary Smith, and David Doss. This work used the Immersion Grating Infrared Spectrograph (IGRINS) that was developed under a collaboration between the University of Texas at Austin and the Korea Astronomy and Space Science Institute (KASI) with the financial support of the US National Science Foundation under grant AST-1229522, of the University of Texas at Austin, and of the Korean GMT Project of KASI.

## REFERENCES

[1] Follert, R., Dorn, R. J., Oliva, E., Lizon, J. L., Hatzes, A., Piskunov, N., Reiners, A., Seemann, U., Stempels, E., Heiter, U., Marquart, T., Lockhart, M., Anglada-Escude, G., Löwinger, T., Baade, D., Grunhut, J., Bristow, P., Klein, B., Jung, Y., Ives, D. J., Kerber, F., Pozna, E., Paufique, J., Kaeufl, H. U., Origlia, L., Valenti, E., Gojak, D., Hilker, M., Pasquini, L., Smette, A., and Smoker, J., "CRIRES+: a cross-dispersed high-resolution infrared spectrograph for the ESO VLT," in [*Ground-based and Airborne Instrumentation for Astronomy V*], *Proc. SPIE,* **9147**, 914719 (July 2014).

[2] Rayner, J., Bond, T., Bonnet, M., Jaffe, D., Muller, G., and Tokunaga, A., "iSHELL: a 1-5 micron cross-dispersed R=70,000 immersion grating spectrograph for IRTF," in [*Ground-based and Airborne Instrumentation for Astronomy IV*], *Proc. SPIE,* **8446**, 84462C (Sept. 2012).

[3] Jaffe, D. T., Barnes, S., Brooks, C., Gully-Santiago, M., Pak, S., Park, C., and Yuk, I., "GMTNIRS (Giant Magellan Telescope Near-Infrared Spectrograph): optimizing the design for maximum science productivity and minimum risk," in [*Ground-based and Airborne Instrumentation for Astronomy V*], *Proc. SPIE,* **9147**, 914722 (July 2014).

[4] McLean, I. S., Becklin, E. E., Bendiksen, O., Brims, G., Canfield, J., Figer, D. F., Graham, J. R., Hare, J., Lacayanga, F., Larkin, J. E., Larson, S. B., Levenson, N., Magnone, N., Teplitz, H., and Wong, W., "Design and development of NIRSPEC: a near-infrared echelle spectrograph for the Keck II telescope," in [*Infrared Astronomical Instrumentation*], Fowler, A. M., ed., *Proc. SPIE,* **3354**, 566–578 (Aug. 1998).

[5] Yuk, I.-S., Jaffe, D. T., Barnes, S., Chun, M.-Y., Park, C., Lee, S., Lee, H., Wang, W., Park, K.-J., Pak, S., Strubhar, J., Deen, C., Oh, H., Seo, H., Pyo, T.-S., Park, W.-K., Lacy, J., Goertz, J., Rand, J., and Gully-Santiago, M., "Preliminary design of IGRINS (Immersion GRating INfrared Spectrograph)," in [*Society of Photo-Optical Instrumentation Engineers (SPIE) Conference Series*], *Society of Photo-Optical Instrumentation Engineers (SPIE) Conference Series* **7735**, 1 (July 2010).

[6] Park, C., Jaffe, D. T., Yuk, I.-S., Chun, M.-Y., Pak, S., Kim, K.-M., Pavel, M., Lee, H., Oh, H., Jeong, U., Sim, C. K., Lee, H.-I., Nguyen Le, H. A., Strubhar, J., Gully-Santiago, M., Oh, J. S., Cha, S.-M., Moon, B., Park, K., Brooks, C., Ko, K., Han, J.-Y., Nah, J., Hill, P. C., Lee, S., Barnes, S., Yu, Y. S., Kaplan, K., Mace, G., Kim, H., Lee, J.-J., Hwang, N., and Park, B.-G., "Design and early performance of IGRINS (Immersion Grating Infrared Spectrometer)," in [*Society of Photo-Optical Instrumentation Engineers (SPIE) Conference Series*], *Society of Photo-Optical Instrumentation Engineers (SPIE) Conference Series* **9147**, 1 (July 2014).

[7] Marsh, J. P., Mar, D. J., and Jaffe, D. T., "Production and evaluation of silicon immersion gratings for infrared astronomy," *Appl Opt.,* **46**, 3400–3416 (June 2007).

[8] Gully-Santiago, M., Wang, W., Deen, C., and Jaffe, D., "Near-infrared metrology of high-performance silicon immersion gratings," in [*Modern Technologies in Space- and Ground-based Telescopes and Instrumentation II*], *Proc. SPIE,* **8450**, 84502S (Sept. 2012).

[9] Frey, B. J., Leviton, D. B., and Madison, T. J., "Temperature-dependent refractive index of silicon and germanium," in [*Society of Photo-Optical Instrumentation Engineers (SPIE) Conference Series*], *Proc. SPIE,* **6273**, 62732J (June 2006).

[10] Kaeufl, H.-U., Ballester, P., Biereichel, P., Delabre, B., Donaldson, R., Dorn, R., Fedrigo, E., Finger, G., Fischer, G., Franza, F., Gojak, D., Huster, G., Jung, Y., Lizon, J.-L., Mehrgan, L., Meyer, M., Moorwood, A., Pirard, J.-F., Paufique, J., Pozna, E., Siebenmorgen, R., Silber, A., Stegmeier, J., and Wegerer, S., "CRIRES: a high-resolution infrared spectrograph for ESO's VLT," in [*Ground-based Instrumentation for Astronomy*], Moorwood, A. F. M. and Iye, M., eds., *Proc. SPIE,* **5492**, 1218–1227 (Sept. 2004).

[11] Lee, J.-E., Park, S., Green, J. D., Cochran, W. D., Kang, W., Lee, S.-G., and Sung, H.-I., "High Resolution Optical and NIR Spectra of HBC 722," *ApJ* **807**, 84 (July 2015).

[12] Gullikson, K., Kraus, A., Dodson-Robinson, S., Jaffe, D., Lee, J.-E., Mace, G. N., MacQueen, P., Park, S., and Riddle, A., "Direct Spectral Detection: An Efficient Method to Detect and Characterize Binary Systems," *AJ,* **151**, 3 (Jan. 2016).

[13] Sterling, N. C., Dinerstein, H. L., Kaplan, K. F., and Bautista, M. A., "Discovery of Rubidium, Cadmium, and Germanium Emission Lines in the Near-infrared Spectra of Planetary Nebulae," *ApJ,* **819**, L9 (Mar. 2016).

[14] Afşar, M., Sneden, C., Frebel, A., Kim, H., Mace, G. N., Kaplan, K. F., Lee, H.-I., Oh, H., Sok Oh, J., Pak, S., Park, C., Pavel, M. D., Yuk, I.-S., and Jaffe, D. T., "The Chemical Compositions of Very Metal-poor Stars HD 122563 and HD 140283: A View from the Infrared," *ApJ,* **819**, 103 (Mar. 2016).

[15] Oh, H., Pyo, T.-S., Yuk, I.-S., Park, B.-G., Park, C., Chun, M.-Y., Pak, S., Kim, K.-M., Sok Oh, J., Jeong, U., Yu, Y. S., Lee, J.-J., Kim, H., Hwang, N., Kaplan, K., Pavel, M., Mace, G., Lee, H.-I., Nguyen Le, H. A., Lee, S., and Jaffe, D. T., "IGRINS Near-IR High-resolution Spectroscopy of Multiple Jets around LkH$\alpha$ 234," *ApJ,* **817**, 148 (Feb. 2016).

[16] Lee, S., Lee, J.-E., Park, S., Lee, J.-J., Kidder, B., Mace, G. N., and Jaffe, D. T., "IGRINS spectroscopy of Class I sources: IRAS 03445+3242 and IRAS 04239+2436," *ArXiv e-prints* (May 2016).

[17] Mann, A. W., Gaidos, E., Mace, G. N., Johnson, M. C., Bowler, B. P., LaCourse, D., Jacobs, T. L., Vanderburg, A., Kraus, A. L., Kaplan, K. F., and Jaffe, D. T., "Zodiacal Exoplanets in Time (ZEIT). I. A Neptune-sized Planet Orbiting an M4.5 Dwarf in the Hyades Star Cluster," *ApJ,* **818**, 46 (Feb. 2016).

[18] Mann, A. W., Newton, E. R., Rizzuto, A. C., Irwin, J., Feiden, G. A., Gaidos, E., Mace, G. N., Kraus, A. L., James, D. J., Ansdell, M., Charbonneau, D., Covey, K. R., Ireland, M. J., Jaffe, D. T., Johnson, M. C., Kidder, B., and Vanderburg, A., "Zodiacal Exoplanets in Time (ZEIT) III: A Neptune-sized planet orbiting a pre-main-sequence star in the Upper Scorpius OB Association," *ArXiv e-prints* (Apr. 2016).

[19] Gaidos, E., Mann, A. W., RIzzuto, A., Nofi, L., Mace, G., Vanderburg, A., Feiden, G., Narita, N., Takeda, Y., Esposito, T. M., De Rosa, R. J., Ansdell, M., Hirano, T., Graham, J. R., Kraus, A., and Jaffe, D., "Zodiacal Exoplanets in Time (ZEIT) II. A "Super-Earth" Orbiting a Young K Dwarf in the Pleiades Neighborhood," *ArXiv e-prints* (June 2016).

[20] Johns-Krull, C. M., McLane, J. N., Prato, L., Crockett, C. J., Jaffe, D. T., Hartigan, P. M., Beichman, C. A., Mahmud, N. I., Chen, W., Skiff, B. A., Cauley, P. W., Jones, J. A., and Mace, G. N., "A Candidate Young Massive Planet in Orbit around the Classical T Tauri Star CI Tau," *ArXiv e-prints* (May 2016).

[21] Le, H. A. N., Pak, S., Jaffe, D. T., Kaplan, K., Lee, J.-J., Im, M., and Seifahrt, A., "Exposure time calculator for Immersion Grating Infrared Spectrograph: IGRINS," *Advances in Space Research* **55**, 2509–2518 (June 2015).

[22] Lee, J.-J., "plp: Version 2.0," (June 2015).

[23] McLean, I. S., Steidel, C. C., Epps, H. W., Konidaris, N., Matthews, K. Y., Adkins, S., Aliado, T., Brims, G., Canfield, J. M., Cromer, J. L., Fucik, J., Kulas, K., Mace, G., Magnone, K., Rodriguez, H., Rudie, G., Trainor, R., Wang, E., Weber, B., and Weiss, J., "MOSFIRE, the multi-object spectrometer for infra-red exploration at the Keck Observatory," in [*Ground-based and Airborne Instrumentation for Astronomy IV*], *Proc. SPIE,* **8446**, 84460J (Sept. 2012).

[24] Kulas, K. R., McLean, I. S., and Steidel, C. C., "Performance of the HgCdTe detector for MOSFIRE, an imager and multi-object spectrometer for Keck Observatory," in [*High Energy, Optical, and Infrared Detectors for Astronomy V*], *Proc. SPIE,* **8453**, 84531S (July 2012).

[25] Jeong, U., Chun, M.-Y., Oh, J. S., Park, C., Yuk, I.-S., Oh, H., Kim, K.-M., Ko, K. Y., Pavel, M. D., Yu, Y. S., and Jaffe, D. T., "Characterization and optimization for detector systems of IGRINS," in [*Society of Photo-Optical Instrumentation Engineers (SPIE) Conference Series*], *Society of Photo-Optical Instrumentation Engineers (SPIE) Conference Series* **9154**, 1 (July 2014).

[26] Finger, G., Dorn, R. J., Meyer, M., Mehrgan, L., Stegmeier, J., and Moorwood, A. F. M., "Performance of large-format 2Kx2K MBE grown HgCdTe Hawaii-2RG arrays for low-flux applications," in [*Optical and Infrared Detectors for Astronomy*], Garnett, J. D. and Beletic, J. W., eds., *Proc. SPIE,* **5499**, 47–58 (Sept. 2004).

[27] Finger, G., Dorn, R. J., Eschbaumer, S., Hall, D. N. B., Mehrgan, L., Meyer, M., and Stegmeier, J., "Performance evaluation, readout modes, and calibration techniques of HgCdTe Hawaii-2RG mosaic arrays," in [*High Energy, Optical, and Infrared Detectors for Astronomy III*], *Proc. SPIE,* **7021**, 70210P (July 2008).

[28] Hinkle, K. H., Blum, R. D., Joyce, R. R., Sharp, N., Ridgway, S. T., Bouchet, P., van der Bliek, N. S., Najita, J., and Winge, C., "The Phoenix Spectrograph at Gemini South," in [*Discoveries and Research Prospects from 6- to 10-Meter-Class Telescopes II*], Guhathakurta, P., ed., *Proc. SPIE,* **4834**, 353–363 (Feb. 2003).

[29] Prato, L., Mace, G. N., Rice, E. L., McLean, I. S., Kirkpatrick, J. D., Burgasser, A. J., and Kim, S. S., "Radial Velocity Variability of Field Brown Dwarfs," *ApJ,* **808**, 12 (July 2015).

[30] Howell, S. B., Sobeck, C., Haas, M., Still, M., Barclay, T., Mullally, F., Troeltzsch, J., Aigrain, S., Bryson, S. T., Caldwell, D., Chaplin, W. J., Cochran, W. D., Huber, D., Marcy, G. W., Miglio, A., Najita, J. R., Smith, M., Twicken, J. D., and Fortney, J. J., "The K2 Mission: Characterization and Early Results," *PASP,* **126**, 398–408 (Apr. 2014).

[31] Sneden, C., "The nitrogen abundance of the very metal-poor star HD 122563.," *ApJ,* **184**, 839–849 (Sept. 1973).

[32] Tielens, A. G. G. M. and Hollenbach, D., "Photodissociation regions. I - Basic model. II - A model for the Orion photodissociation region," *ApJ,* **291**, 722–754 (Apr. 1985).

[33] Burton, M. G., Hollenbach, D. J., and Tielens, A. G. G. M., "Line emission from clumpy photodissociation regions," *ApJ,* **365**, 620–639 (Dec. 1990).

[34] Parmar, P. S., Lacy, J. H., and Achtermann, J. M., "Detection of low-J pure-rotational emission from H2 in the Orion Bar region - Evidence for small-scale clumpiness," *ApJ,* **372**, L25–L28 (May 1991).

[35] Allers, K. N., Jaffe, D. T., Lacy, J. H., Draine, B. T., and Richter, M. J., "$H_2$ Pure Rotational Lines in the Orion Bar," *ApJ,* **630**, 368–380 (Sept. 2005).

[36] Pellegrini, E. W., Baldwin, J. A., Ferland, G. J., Shaw, G., and Heathcote, S., "Orion's Bar: Physical Conditions Across the Definitive $H^+/H^0/H_2$ Interface," *ApJ,* **693**, 285–302 (Mar. 2009).

[37] Shaw, G., Ferland, G. J., Henney, W. J., Stancil, P. C., Abel, N. P., Pellegrini, E. W., Baldwin, J. A., and van Hoof, P. A. M., "Rotationally Warm Molecular Hydrogen in the Orion Bar," *ApJ,* **701**, 677–685 (Aug. 2009).

[38] Lee, S., Yuk, I.-S., Lee, H., Wang, W., Park, C., Park, K.-J., Chun, M.-Y., Pak, S., Strubhar, J., Deen, C., Gully-Santiago, M., Rand, J., Seo, H., Kwon, J., Oh, H., Barnes, S., Lacy, J., Goertz, J., Park, W.-K., Pyo, T.-S., and Jaffe, D. T., "GMTNIRS (Giant Magellan Telescope near-infrared spectrograph): design concept," in [*Ground-based and Airborne Instrumentation for Astronomy III*], *Proc. SPIE,* **7735**, 77352K (July 2010).

[39] Jaffe, D. T., Mar, D. J., Warren, D., and Segura, P. R., "GMTNIRS: the high resolution near-IR spectrograph for the Giant Magellan Telescope," in [*Society of Photo-Optical Instrumentation Engineers (SPIE) Conference Series*], *Proc. SPIE,* **6269**, 62694I (June 2006).

[40] Brooks, C., "Process improvements in the production of silicon immersion gratings," in [*Coatings, Filters and Gratings I*], *Proc. SPIE,* **9912** (Sept. 2016).

[41] Kidder, B., "Approaching perfection in the manufacturing of silicon immersion gratings," in [*Coatings, Filters and Gratings I*], *Proc. SPIE,* **9912** (Sept. 2016).

[42] Skrutskie, M. F., Cutri, R. M., Stiening, R., Weinberg, M. D., Schneider, S., Carpenter, J. M., Beichman, C., Capps, R., Chester, T., Elias, J., Huchra, J., Liebert, J., Lonsdale, C., Monet, D. G., Price, S., Seitzer, P., Jarrett, T., Kirkpatrick, J. D., Gizis, J. E., Howard, E., Evans, T., Fowler, J., Fullmer, L., Hurt, R., Light, R., Kopan, E. L., Marsh, K. A., McCallon, H. L., Tam, R., Van Dyk, S., and Wheelock, S., "The Two Micron All Sky Survey (2MASS)," *AJ,* **131**, 1163–1183 (Feb. 2006).

[43] Jaffe, D., "GMTNIRS: progress toward the Giant Magellan Telescope near- infrared spectrograph," in [*Instruments for Extremely Large Telescopes II*], *Proc. SPIE,* **9908** (Sept. 2016).